TOPICAL REVIEW — ZNO-RELATED MATERIALS AND DEVICES

Recent progress of ZnMgO ultraviolet photodetector

To cite this article: Jia-Lin Yang *et al* 2017 *Chinese Phys. B* **26** 047308

TOPICAL REVIEW — ZnO-related materials and devices

Recent progress of ZnMgO ultraviolet photodetector*

Jia-Lin Yang(杨佳霖)[1,2], Ke-Wei Liu(刘可为)[1,†], and De-Zhen Shen(申德振)[1]

[1] State Key Laboratory of Luminescence and Applications, Changchun Institute of Optics, Fine Mechanics and Physics, Chinese Academy of Sciences, Changchun 130033, China

[2] University of Chinese Academy of Sciences, Beijing 100049, China

(Received 1 November 2016; revised manuscript received 8 December 2016; published online 10 March 2017)

The ultra-violet (UV) detection has a wide application in both civil and military fields. ZnO is recognized as one of ideal materials for fabricating the UV photodetectors due to its plenty of advantages, such as wide bandgap, low cost, being environment-friendly, high radiation hardness, etc. Moreover, the alloying of ZnO with MgO to make ZnMgO could continually increase the band gap from ∼ 3.3 eV to ∼ 7.8 eV, which allows both solar blind and visible blind UV radiation to be detected. As is well known, ZnO is stabilized in the wurtzite structure, while MgO is stabilized in the rock salt structure. As a result, with increasing the Mg content, the crystal structure of ZnMgO alloy will change from wurtzite structure to rock salt structure. Therefore, ZnMgO photodetectors can be divided into three types based on the structures of alloys, namely, wurtzite-phase, cubic-phase and mixed-phase devices. In this paper, we review recent development and make the prospect of three types of ZnMgO UV photodetectors.

Keywords: ZnO, ZnMgO, UV, photodetector

PACS: 73.61.Ga, 85.60.Gz **DOI:** 10.1088/1674-1056/26/4/047308

1. Introduction

The UV photodetectors have been widely used in both civil and military applications, such as space probing, missile early-warning, flame detecting and UV monitoring.[1–3] Nowadays the main parts of commercial UV photodetectors are Si-based photodiodes and vacuum photomultipliers for their advantages of relatively mature technology. Although they have low noise and fast response speed, many significant limitations exist. For instance, to reduce the influence of long-wavelength light, Si-based photodiodes operated as UV photodetectors usually need filters. And vacuum photomultipliers always require an ultra-high vacuum environment and a high voltage. In addition, the performances of these devices degrade obviously during long-term UV illumination.

As the study on wide bandgap semiconductors (i.e., GaN, SiC, and ZnO) develops in depth, it is found that UV photodetectors based on wide bandgap semiconductors have special advantages, such as high radiation hardness, intrinsic visible blind, low working voltage, and high stability, and so on.[4,5] Compared with other wide bandgap materials, GaN-based materials possess plenty of unique advantages, and have been regarded as the most promising materials for UV detection. For instance, GaN has large direct bandgap (3.4 eV), high electron saturation drift velocity (2.7×10^7 cm/s), and high chemical stability.[6] And the bandgap of GaN-based materials can be modulated from 3.4 eV to 6.2 eV continuously by alloying GaN with Al.[7,8] In addition, the relatively mature growth technology of GaN, especially for fabricating the P-type materials, makes GaN-based UV photodetectors far ahead of the devices based on other wide bandgap materials.[9,10] Nevertheless, GaN-based materials are usually fabricated on sapphire substrates, and a large lattice mismatch between them often leads to a high density of defects.[11] Additionally, the fabrication of high quality P-type GaAlN with high Al content is still a big challenge.[12,13] Recently, ZnO-based materials have attracted more and more attention. Compared with GaN-based materials, ZnO-based materials have many impressive advantages, such as lower density of defects, being environmental friendly and stronger radiation hardness.[14,15] Moreover, alloying ZnO with MgO in varying amounts could increase the bandgap of ZnO from 3.37 eV to 7.8 eV. Therefore, ZnO and its ternary alloy ZnMgO each have a great potential application in UV detections. Although the lack of reliable P-type materials hinders the PN-junction photodetectors from being further utilized, the ZnO-based devices with metal–semiconductor–metal (MSM) and Schottky structures are still attractive due to their excellent performance.

In 2010, the first review focused on the ZnO-based semiconductor UV photodetectors was published by Liu *et al.*, and the history and the development of ZnO-based photodetectors can be obtained.[16] Recently, the performances of ZnO-based UV photodetectors and the relevant physics are given by Hou *et al.*[17] In the previous reviews, ZnO-based UV photodetectors are usually classified according to the device structure.

*Project supported by the National Natural Science Foundation of China (Grant No. 61475153) and the 100 Talents Program of the Chinese Academy of Sciences.

†Corresponding author. E-mail: liukw@ciomp.ac.cn

As is well known, ZnO is stabilized in the hexagonal wurtzite structure, while MgO is stabilized in the cubic rock salt structure. (Figs. 1(a) and 1(b)). As a result, with increasing the Mg content as shown in Fig. 1(c), the crystal structure of ZnMgO alloy will change from wurtzite structure (w-ZnMgO) to cubic structure (c-ZnMgO).[18] Notably, the coexistence of two structures in ZnMgO seems to be unavoidable in the structure transformation process, and this ZnMgO with both hexagonal and cubic phase is usually called mixed-phase ZnMgO (m-ZnMgO). Therefore, ZnMgO photodetectors can be divided into three types based on the structure of alloys, namely, w-ZnMgO, c-ZnMgO, and m-ZnMgO devices. The performance of ZnMgO photodetectors is strongly dependent on the alloy structure.

In this article, we firstly review the ZnMgO UV photodetectors classified according to the material structure (c-, w-, and m-ZnMgO films) in recent five years. Following this, we will give an outlook on future direction in the field of ZnO-based UV photodetectors.

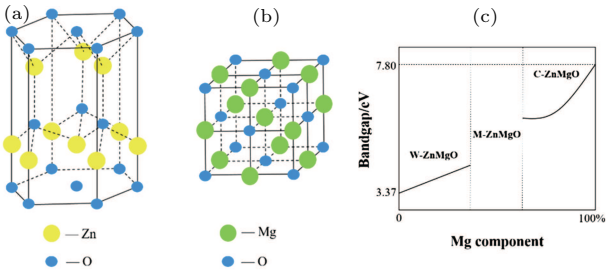

Fig. 1. (color online) Schematic diagrams of (a) wurtzite structure and (b) rock salt structure. (Blue spheres represent O atoms, yellow spheres represent Zn atoms and green ones represent Mg atoms.) (c) Schematic diagram of the variation of bandgap and lattice structure with Mg component.

2. Wurtzite-ZnMgO photodetectors

Wurtzite structure is the most stable type for ZnO, and thus w-ZnMgO has attracted much attention for the purpose of bandgap engineering, manipulating electronic and optical properties of ZnO.[19–21] The fabrication and investigation of high quality ZnMgO films were first reported in 1998 by Ohtomo *et al.*[22] They have grown a series of high quality w-ZnMgO films by pulsed laser deposition (PLD). Since then, more and more researches on ZnMgO materials have been reported.[23–25] Various methods have been utilized to synthesize the ZnMgO films, such as sputtering, PLD, molecular beam epitaxy (MBE), metal organic chemical vapor deposition (MOCVD), Sol-Gel, etc.

As mentioned in Section 1, ZnMgO films are widely used as UV photodetectors. The first w-ZnMgO UV photodetector was fabricated in 2001 by Yang *et al.*[26] Since then, a number of w-ZnMgO UV photodetectors have been reported in succession.[27–29] To a great extent, the performance of a ZnMgO UV photodetector usually depends on the quality of ZnMgO film itself. In recent five years, people have used different fabrication methods (mainly sputtering[30–34] and MBE[35,36]) to prepare the ZnMgO films under various growth conditions. Sputtering is a very simple and cheap method of growing the ZnMgO alloys, and the composition of the alloy is very easy to control.[37–39] Recently, Tang *et al.* found that the increasing sputtering power of MgO target could increase ZnMgO bandgap.[30] Additionally, Li *et al.* found that the proper oxygen flow rate could increase the responsivity of ZnMgO photodetector.[33] Compared with the sputtering method, MBE method is expensive, but the ZnMgO film fabricated by MBE presents higher quality than by sputtering. Schoenfeld *et al.* have grown ZnO nucleation layers and ZnO buffer layers in order to grow high quality w-ZnMgO films.[36] Then they investigated the influences of different growth conditions (growth temperature, Zn cell temperature, oxygen flow rate and RF power) on the performances of the three layers (ZnO nucleation layers, ZnO buffer layers and w-ZnMgO layers).

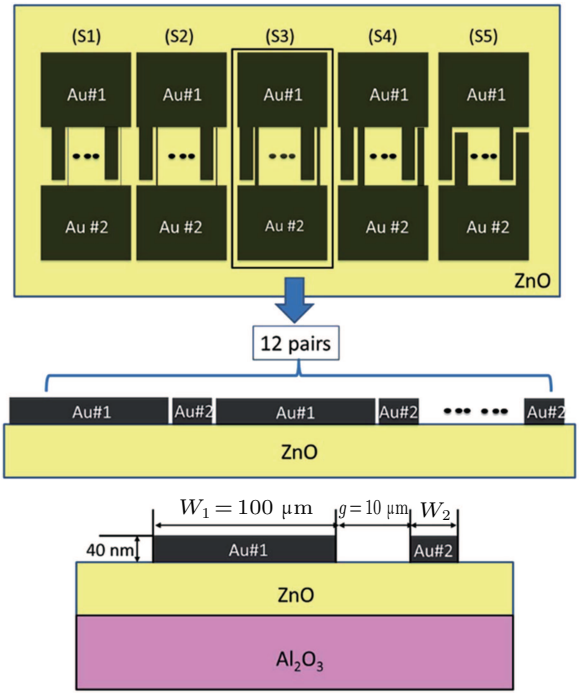

Fig. 2. (color online) Schematic diagram of asymmetric electrodes and MSM photodetectors.[42]

In order to improve the performance of w-ZnMgO photodetector, various methods have been selected in recent five years, such as the post-annealing process,[40,41] the new electrode structure,[42] surface treatment,[43] etc.[44,45] Hou *et al.* have improved the peak responsivity of w-ZnMgO photodetector from 0.22 A/W to 1 A/W by 400 °C annealing in argon atmosphere.[40] Chen *et al.* have investigated the influence of the electrode structure on the performance of MSM photodetector.[42] They found that the MSM devices with asymmetric Au electrodes can work without biases. The schematic structures of the asymmetric electrodes are shown in Fig. 2: one Au interdigitated electrode with wide fingers

and the other one with narrow fingers. Interestingly, with increasing the asymmetric ratio (the ratio between the width of wide fingers and the width of narrow fingers) of the interdigitated electrodes, the responsivity of the ZnO self-powered UV photodetectors was enhanced obviously, reaching as high as 20 mA/W when the asymmetric ratio was 20:1. The origin of the photoresponse at 0 V should be associated with the asymmetric electric potential distribution in ZnO film and the accumulated and trapped holes at the Au/ZnO interfaces. The findings in this work provide a new route to realizing self-powered photodetectors.

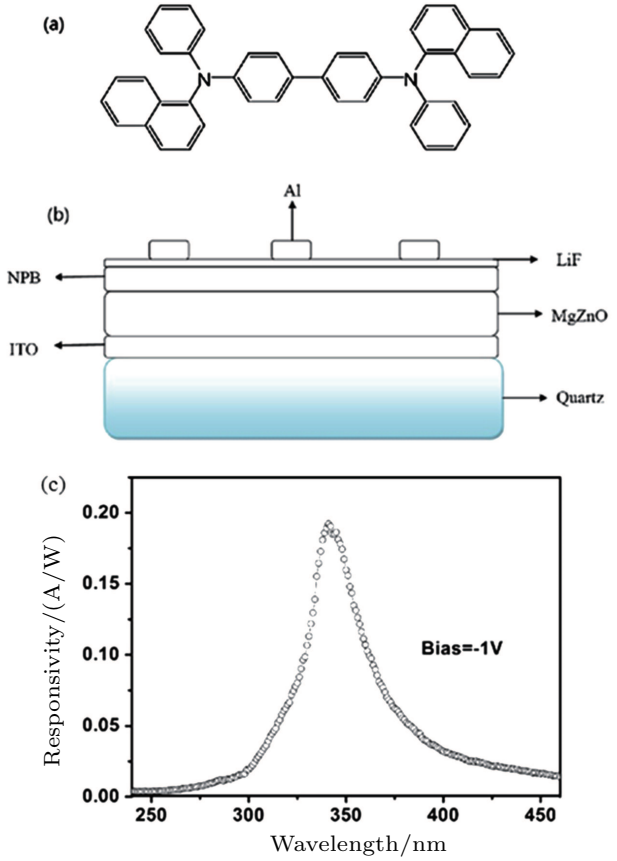

Fig. 3. (color online) (a) Structure of NPB. (b) Schematic diagram of ZnMgO PN-heterojunction photodetector with P-type organic semiconductor. (c) Responsivity curve of the photodetector.[46]

PN-junction photodetector is supposed to be the most suitable choice for future applications in consequence of its fast responding speed, low dark current, and working without applied bias. However, P-type doping is still a big challenge to ZnO-based semiconductor. Thus, P-type organic semiconductor has been taken into account to realize PN-heterojunction photodetector on ZnO-based film.[48,49] In 2012, N, N'-bis (naphthalen-1-y1)-N, N'-bis (pheny)ben-zidine (NPB), which is usually used as hole transporting layer for its high hole mobility of (2–4)$\times 10^{-4}$ cm^2/(V·s) and hole concentration of $\sim 10^{14}$ cm^{-3}, was selected to fabricate a heterojunction photodetector by Hu *et al.* (Fig. 3(a)).[46] The dark *I*–*V* curve of the detector indicated that the device has a good rectifying property and a relatively low dark current (I_d: 3×10^{-10} A). The responsivity of this device was 0.192 A/W at 340 nm and −1-V bias (Fig. 3(c)). Just as mentioned above, the fabrication of high quality, stable and repeatable P-type ZnO-based film still faces a big challenge, but great progress has been made through persistent efforts.[50–52] In 2015, Shan *et al.* used MBE to prepare high quality p-type films by employing the Li, N co-doping method. The hole concentration and Hall mobility were 3.6×10^{16} cm^3 and 3.2 cm^2/(V·s), respectively.[47] Based on this, P-ZnMgO/I-ZnO/N-ZnO quasi-homojunction detectors were demonstrated with a cutoff wavelength of 379 nm. The *I*–*V* curve of the device showed obvious rectifying diode behavior in a dark environment with a turn-on voltage of around 6.2 V (Fig. 4). The peak responsivity at 362 nm increased linearly from 7.8×10^{-4} A/W to 0.22 A/W with increasing the bias from 0 V to 5 V. The rise time of detectors was 0.32 ms and the fall time was less than 10 ms.

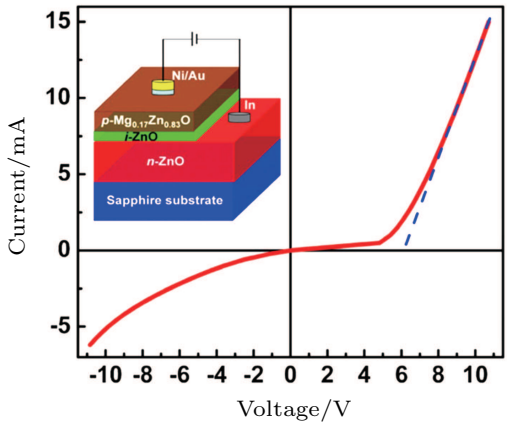

Fig. 4. (color online) *I*–*V* curve of P-ZnMgO/I-ZnO/N-ZnO quasi-homojunction detector. The insert is the schematic diagram of the device structure.[47]

As is well known, the ozone layer in the upper atmosphere can block a part of UV radiation from the sunlight with the wavelength between 220 nm and 280 nm, which is thus usually called solar-blind UV region. Therefore, without any interference from the sun, solar-blind UV photodetector has a higher accuracy and sensitivity, which can work in all weather. For w-ZnMgO film materials as mentioned in Section 1, phase separation appears naturally when the components of Zn and Mg are similar (Fig. 1(c)). Therefore, it is difficult to realize high quality single phase w-ZnMgO solar UV photodetectors.

In order to extend the band gap of w-ZnMgO into the solar-blind region, different methods have been selected.[53] Using a suitable substrate or buffer layer is an effective way to avoid phase separation. In 2011, Zheng *et al.* prepared $Zn_{0.51}Mg_{0.49}O$ on the ZnO substrates by reactive magnetron co-sputtering method. Only one peak was observed around 260 nm with a peak responsivity of 304 mA/W at 10-V bias.[54] Recently, a high quality single phase $Zn_{0.54}Mg_{0.46}O$ film was successfully fabricated by Schoenfeld *et al.* on the sapphire substrate by introducing a ZnO buffer layer through

using the rf-MBE.[36] Based on this film, Schottky photodetector has been demonstrated with a dark current of 2.7 μA at 5-V bias. The device showed a solar-blind UV response with a response peak at 265 nm. And the peak responsivity at 5-V bias was 201 A/W (see Fig. 5), which has been the highest responsivity of w-ZnMgO solar-blind UV photodetectors up to now. It is worth noting that a shoulder appeared near 310 nm–375 nm in the response spectrum, which should be related to the ZnO buffer layer.

Just as mentioned above, ZnO substrate or buffer layer usually has a response in the visible blind UV region, which could reduce the performance of solar blind UV photodetector. In order to resolve this problem, Liang *et al.* firstly grew a thin Be film on the Si substrate and a high Mg content w-ZnMgO film was subsequently prepared on it by rf-MBE.[55] In the process of preparing film, Be was oxidized into BeO, which is wurtzite structure serving as a buffer layer in favor of preventing phase separation of the w-ZnMgO film. Finally, a ZnMgO/BeO/p-Si heterojunction detector was fabricated. The *I*–*V* curve of the device displayed a good rectification as shown in Fig. 6(a). The dark current was 2 nA at −3-V bias and the rectification ratio was about 300 at ±3 V. The cutoff wavelength was 280 nm and the peak responsivity was 11 mA/W at 0.5-V bias (Fig. 6(b)). After that, some other researches about BeO buffer layers were also reported.[56,57]

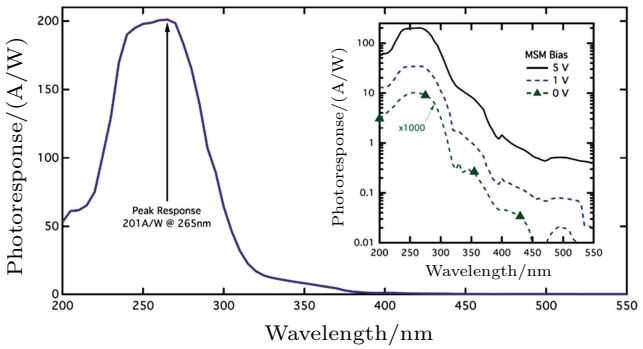

Fig. 5. (color online) Responsivity of $Zn_{0.54}Mg_{0.46}O$ MSM photodetector with 10-μm finger gap at 5-V bias. The inset shows the log plot of the responsivity curve at different biases.[36]

In brief, introducing a ZnO or BeO buffer layer is an effective and common method to synthesize high quality w-ZnMgO film with the band gap in the solar blind region. However, some disadvantages still exist. ZnO buffer layer usually produces additional response in the visible blind UV region, and BeO has strong toxicity, which is harmful to both humans and the environment. Besides, w-$Zn_{1-x}Mg_xO$ films with x exceeding 0.55 have not been reported so far to our knowledge. Other efforts were also made to prepare high Mg-component single phase w-ZnMgO film, such as using high Mg component ZnMgO targets in sputtering methods,[41,58] increasing Mg RF power with two pure metal targets(Mg and Zn),[59] or utilizing annealing treatment.[60] But these methods still need further investigating. Therefore, more efforts need to be made to fabricate the high Mg content w-ZnMgO.

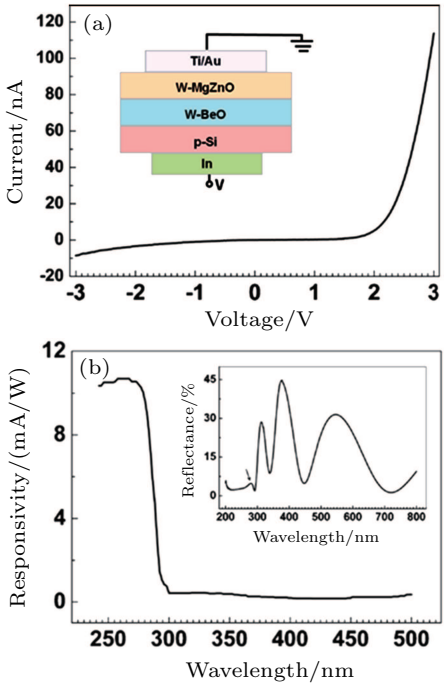

Fig. 6. (color online) (a) *I*–*V* curve of high Mg component w-ZnMgO/BeO/Si heterojunction detector. The inset shows the schematic diagram of the device. (b) Response spectrum of the device. The inset is the reflectance spectrum. (reproduced from Ref. [55], with the permission of AIP Publishing.)[55]

3. Cubic-ZnMgO photodetectors

In Fig. 1(c), it can be clearly found that the bandgap of c-ZnMgO is larger than that of w-ZnMgO. Additionally, according to the phase diagram of MgO-ZnO, solid solubility of ZnO in MgO is higher than that of MgO in ZnO, so the tuning of the composition and the bandgap of c-ZnMgO should be easier. Therefore, c-ZnMgO films have been widely investigated for the applications in solar blind UV photodetectors.[61–63]

In 2014, Schoenfeld *et al.* have grown a series of high quality c-ZnMgO films on the c-face sapphire substrates by MBE through using MgO as buffer layers.[36] The effects of the growth conditions (such as oxygen plasma power, oxygen flow and Mg cell temperature) on the properties of ZnMgO films and their photodetectors have been investigated. It can be found that the roughness and the bandgap of the film decreased with increasing the oxygen plasma power, while the growth rate and responsivity increased. When the oxygen plasma power was above 375 W, phase separation appeared. With the increase of oxygen flow rate from 0.5 sccm to 2.5 sccm, the growth rate increased, while the bandgap of ZnMgO decreased without any phase separation. Increasing Mg cell temperature could increase the roughness, Mg concentration and the growth rate of ZnMgO films. And when Mg cell temperature was set to be between 350 °C and 370 °C, phase separation appeared. Based on these ZnMgO films, the MSM

photodetectors were fabricated and investigated. It could be found that the increase of plasma power or the decrease of Mg cell temperature can increase the responsivity of the device. In addition, increasing the oxygen flow rate could also increase the responsivity slightly. After that, Tian *et al.* grew c-ZnMgO films on quartz substrates by RF magnetron sputtering method.[41] And they have investigated the influence of annealing treatment on the properties of c-ZnMgO film and the corresponding photodetector. They found that Mg component decreased slightly after annealing at 500 °C. Interestingly, the device based on the as-grown c-ZnMgO did not show any photoresponse, but the annealed c-ZnMgO photodetector had an obvious response to solar-blind UV light with a peak responsivity of 0.53 mA/W at about 250 nm. Recently, Fan *et al.* have grown a c-ZnMgO film with a bandgap of 3.9 eV on a-face sapphire using a thin ZnMgO buffer layer by MBE.[64] To our knowledge, its bandgap is narrower than any other bandgap of c-ZnMgO film reported till now. Au interdigital electrodes with different finger gaps (g) were fabricated on c-ZnMgO film to realize MSM structure photodetectors. The dark currents of the devices with $g = 2$ μm, 5 μm, and 10 μm were 3 pA, 2.3 pA, and 1.7 pA at 10 V, respectively. All devices showed a response peak at about 302 nm with a cut-off edge around 320 nm, indicating that the devices were UVB photodetectors (Fig. 7(a)). The peak responsivities of the devices with $g = 2$ μm, 5 μm, and 10 μm were 5.188, 0.428, and 0.022 A/W at 10 V, respectively. The maximum values of responsivity were linearly related to the bias from 10 V to 30 V for all devices (Fig. 7(b)). And the slope of peak responsivity as a function of voltage was inversely proportional to the square of the finger gap as shown in Fig. 7(c). In addition, the peak responsivity was 31.575 A/W at 30-V bias with $g = 2$ μm, corresponding to an internal gain of about 127. And its fall time from 90% to 10% was about 24 μs.

Owing to the small lattice mismatch between c-ZnMgO and MgO, Han *et al.* have attempted to grow c-ZnMgO films on the MgO substrates to improve the crystal quality by MOCVD in 2011.[65] The peak responsivity was 129 mA/W at 238 nm at 15-V bias. And the cutoff wavelength was 253 nm, with the rejection ratio ($R_{24\ 0\mathrm{nm}}/R_{400\ \mathrm{nm}}$) about 4 orders of magnitude. After that, Boutwell *et al.* have grown c-ZnMgO films on the MgO substrates by MBE.[66] The effects of substrate temperature and Mg source flux on the properties of c-ZnMgO films have been investigated. The phase separation appeared with the substrate temperature below 475 °C or with the Mg cell temperature lower than 360 °C. With increasing the substrate temperature from 400 °C to 500 °C, Mg component of c-ZnMgO increased and the crystal quality turned better. It was explained that at a high substrate temperature Zn may be desorbed from the substrate surface before it can be stably bonded into the crystal because the enthalpy of formation for ZnO is lower than that for MgO. On the other hand, when Mg source temperature increased to 360 °C, the defects and the grain boundaries of c-ZnMgO films decreased, leading to the response speed rising dramatically. Nevertheless, the responsivity decreased with increasing the substrate temperature or Mg source flux.

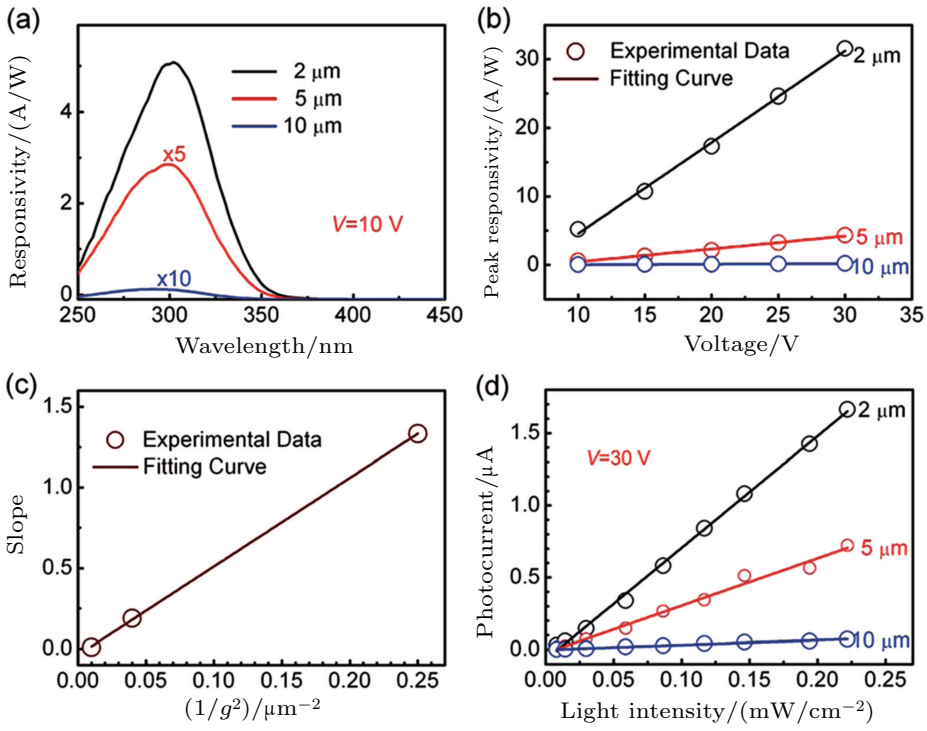

Fig. 7. (color online) (a) Responsivities of the MSM detectors with different finger gaps at 10-V bias. (b) Peak responsivity as a function of the bias on the devices with different finger gaps. (c) Slope of the plot in panel (b) as a function of $1/g^2$. (d) Photocurrents as a function of light intensity with different finger gaps at 30-V bias.[64]

Although c-ZnMgO photodetectors have unique advantages, such as easy-to-realize solar-blind devices and low dark current, the relatively low responsivity hinders them from being practically applied.[63,67] In 2014, Xie *et al.* increased the responsivity of c-ZnMgO photodetector by means of Ga doping through using MOCVD.[68] The responsivity of Ga-doped device was 50 times higher than that of the undoped one at 265 nm under 10-V bias. Subsequently, they have also reported a C-ZnMgO/I-MgO/P-Si solar blind photodetector with high gain via constructing graded-band-gap.[69] The device showed significant rectifying characteristics in dark with a turn-on voltage of about 2 V. The peak responsivity at 240 nm was 1160 mA/W with a cutoff wavelength of about 280 nm at 6-V reverse bias (Fig. 8(b)). And the corresponding quantum efficiency was around 600%. The fall time was gradually shortened with increasing bias. As the bias was beyond 4 V, the fall time was stabilized at about 15 μs due to carriers reaching their saturation velocity.

In short, c-ZnMgO has big potential applications as solar-blind UV photodetectors. However, compared with w-ZnMgO films, the c-ZnMgO films are investigated very rarely. And although various methods have been used to improve the responsivity, the realization of c-ZnMgO photodetector with high responsivity is still a big challenge. In consequence, studies on c-ZnMgO film photodetectors still have a long way to go.

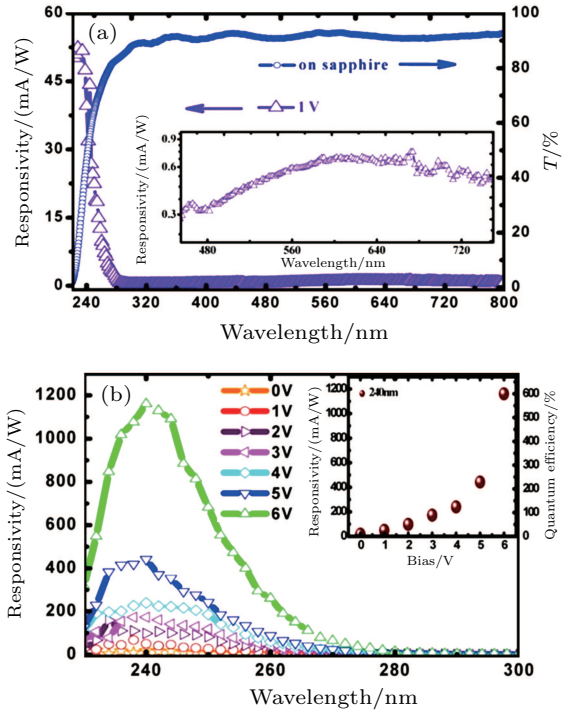

Fig. 8. (color online) (a) Responsivity curve and transmission spectrum of the C-ZnMgO/I-MgO/P-Si photodetector. (b) Responsivity curves with different external biases.[69]

4. Mixed-phase ZnMgO photodetectors

Large efforts have been devoted to the fabrication of high quality single phase ZnMgO film in past years. M-ZnMgO was regarded as byproducts of high quality single phase ZnMgO films. Notablely, the difference in bandgap c- and w-ZnMgO are usually very large due to the fact that two phases have different crystal structures and Zn/Mg ratios. Based on this property, dual-band m-ZnMgO UV photodetectors have been demonstrated by different methods.[70,71]

In 2012, Xie *et al.* reported a dual-band UV photodetector based on m-ZnMgO/I-MgO/P-Si double heterojunction, which is fabricated by MOCVD.[72] The *I–V* curve showed obvious rectifying characteristics with a threshold voltage of about 2 V. Two response bands were observed in solar-blind (∼ 250 nm) and visible-blind (∼ 330 nm) regions, respectively. With increasing the reverse bias from 0 to 1.5 V, the peak in the visible-blind region shifted from 325 nm to 350 nm and the responsivity increased gradually. As for the peak in the solar-blind region, the position and the responsivity only showed a little change at different reserve bias voltages. In the process of research on growing high quality c-ZnMgO film by MBE method, Schoenfeld *et al.* have also reported a series of m-ZnMgO UV photodetectors as byproducts of c-ZnMgO devices.[36] They found that when oxygen plasma power was lower than 375 W, or Mg cell temperature was below 370 °C, or growth temperature was below 475 °C, phase segregation appeared. It is noteworthy that the responsivities of these m-ZnMgO photodetectors in solar-blind region were much higher than (3∼5 orders of magnitude) those of c-ZnMgO ones, though they also had strong response in visible-blind region. When Mg cell temperature was 325 °C, the peak responsivity in the solar-blind region at 1-V bias was up to 462 A/W (Fig. 9(a)).

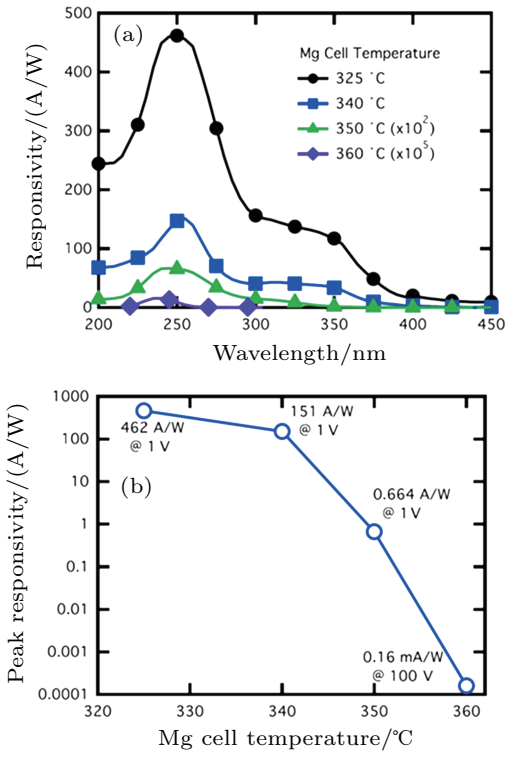

Fig. 9. (color online) (a) Responsivities of m-ZnMgO photodetectors at different Mg cell temperatures. (b) Peak responsivity varies with Mg cell temperature.[36]

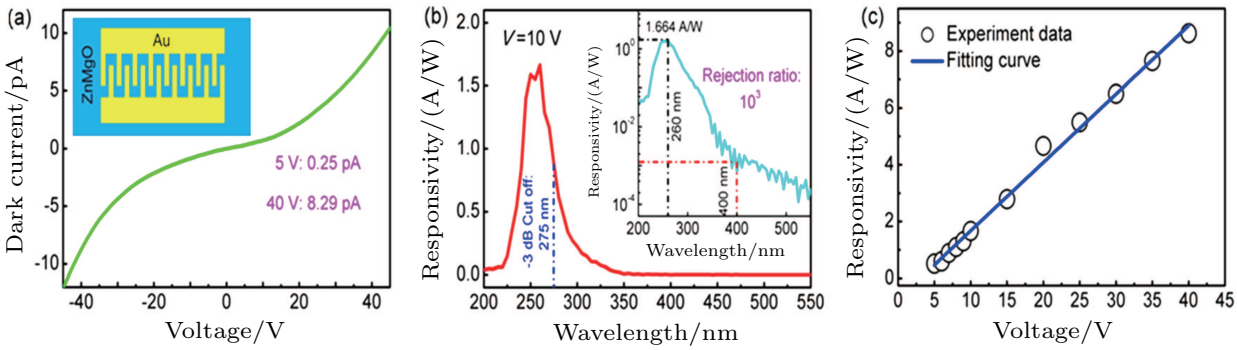

Fig. 10. (color online) (a) *I–V* curve of m-ZnMgO MSM detector. The inset shows the schematic diagram of the device. (b) Response spectrum of the m-ZnMgO detector with single response. The inset shows the spectral response on a logarithmic scale. (c) Peak responsivity as a function of increasing bias.[73]

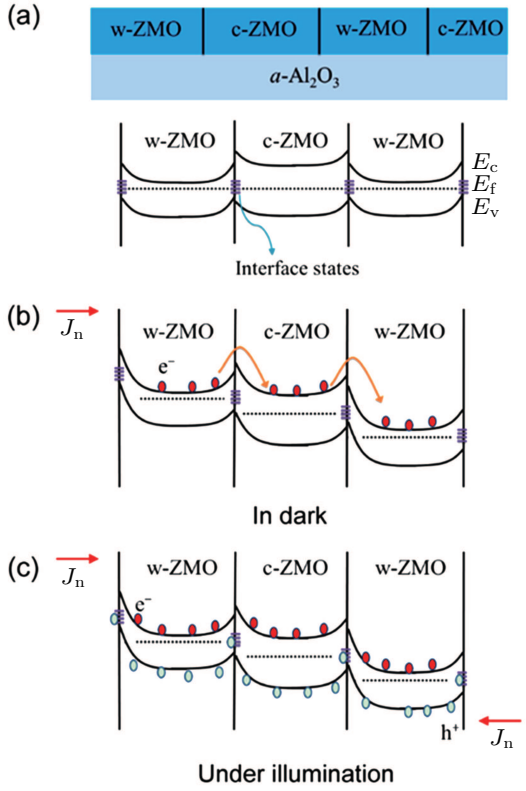

Fig. 11. (color online) Energy band diagram and carrier transport process of m-ZnMgO photodetector under different conditions: (a) in thermal equilibrium, (b) under bias in dark, and (c) under bias with UV illumination.[74]

Owing to a large difference in bandgap between c- and w-ZnMgO, m-ZnMgO usually has two obvious absorption edges: one is shorter than 280 nm and the other is longer than 300 nm, indicating that it is not suitable for solar-blind detection without external filter. Therefore, the investigation of high performance m-ZnMgO UV photodetectors with single cutoff wavelength in solar-blind region is required. By analyzing the previous results, it can be found that two absorption edges of m-ZnMgO should be strongly associated with their growth substrates. More recently, using a-face sapphire (a-Al_2O_3) as a substrate, Fan *et al.* have successfully demonstrated high-performance m-ZnMgO UV photodetector with a single cutoff wavelength in solar-blind UV region for the first time.[73] The dark current was 0.25 pA at 5 V (Fig. 10(a)), which was much lower than those of the most ZnMgO detectors reported before. The single cutoff wavelength was observed to be about 275 nm, and the peak responsivity at 260 nm was about 1.664 A/W at 10 V as shown in the response spectrum (Fig. 10(b)). Moreover, the rejection ratio ($R_{260\ \mathrm{nm}}/R_{400\ \mathrm{nm}}$) was more than 3 orders of magnitude. The peak responsivity increased linearly with the bias rising from 5 V to 40 V (Fig. 10(c)). Subsequently, they went deeper into high performance single response m-ZnMgO UV photodetectors.[74] By means of changing Mg source temperature of MBE, they fabricated a series of m-ZnMgO UV photodetectors with the cutoff wavelengths tuning from 280 nm to 330 nm. All the devices had low dark currents and high responses. The schematic diagrams reasoning the low dark current and high responsivity are shown in Fig. 11. Large amounts of heterojunctions between w-ZnMgO and c-ZnMgO in the m-ZnMgO film should be the reason for the ultra-low dark current. Under the radiation of UV light, photogenerated holes are trapped at the interfaces between w-ZnMgO and c-ZnMgO, prolonging their lifetimes. The longer lifetime could increase the internal gain and then increase the responsivity. The realization of high performance m-ZnMgO photodetectors with single cutoff wavelength has shown a promising prospect in solar and visible blind UV photodetectors. It has profound significance in the field of ZnO-based UV photodetectors. The performances of w-ZnMgO, c-ZnMgO, and m-ZnMgO photodetectors reported in recent five years are summarized in Table 1. In Table 1, it can be found that low dark current and high responsivity make the m-ZnMgO UV photodetectors stand out among the three kinds of devices introduced in this review. Meanwhile, the response time of m-ZnMgO UV photodetector is longer than that of c-ZnMgO device, but is shorter than that of w-ZnMgO device. Till now, quite few studies on m-ZnMgO have been reported to our knowledge. Therefore, more theoretical and experimental researches are demanded in the future.

Table 1. Dark currents, peak responsivities, cutoff wavelengths, rejection ratios, rise times, and decay times of w-, c-, and m-ZnMgO UV photodetectors in recent five years. ("–" denotes "not clear" or "not mentioned" in the article).

	Dark current/pA	Peak responsivity/(A/W)	Cutoff wavelength/nm	Rejection ratio	Rise time (10%–90%)/μs	Fall time (90%–10%)/μs	Ref.
w-ZnMgO	7.67×10^3 (5 V)	34.02	310	2659.7	44.48	1.202×10^5	[31]
w-ZnMgO	0.73 (5 V)	2.133 (10 V)	~ 350	5.46×10^5	$\sim 2\times10^8$	$\sim 6\times10^7$	[33]
w-ZnMgO	40 (10 V)	–	~ 350	~ 4800	2.8×10^7	4×10^6	[34]
w-$Zn_{0.6}Mg_{0.4}O$	700 (–3 V)	0.22 (–2 V)	~ 300	$\sim 10^2$	–	1×10^6	[40]
w-$Zn_{0.6}Mg_{0.4}O$	1.9×10^3 (–3 V)	1 (–2 V)	~ 300	$\sim 10^2$	–	10^8	[40]
w-$Zn_{0.17}Mg_{0.83}O$	5×10^9 (–10 V)	0.22 (5 V)	379	–	320	10^4	[47]
w-$Zn_{0.5}Mg_{0.5}O$	2×10^3 (–3 V)	0.013(1 V) 0.006 (–2 V)	208 301	$\sim 10^2$	10^5	10^5	[56]
w-$Zn_{0.54}Mg_{0.46}O$	–	3.4 (10 V)	280	–	–	482	[59]
c-$Zn_{0.51}Mg_{0.49}O$	3 (10 V)	5.188 (10 V)	320		–	24	[64]
c-$Zn_{0.48}Mg_{0.52}O$	16 (15 V)	0.129 (15 V)	253	$\sim 10^4$	–	1.67	[65]
c-ZnMgO	$\sim 2\times10^5$ (–9 V)	1.160 (6 V)	280	$\sim 10^2$	15	–	[69]
m-$Zn_{0.38}Mg_{0.62}O$	8.29 (40 V)	1.664 (10 V)	275	$\sim 10^3$	–	$1\text{-}2\times10^6$	[73]
m-$Zn_{0.67}Mg_{0.33}O$	78 (40 V)	434 (40 V)	330	$\sim 10^5$	–	3.7×10^4	[74]
m-$Zn_{0.59}Mg_{0.41}O$	11 (40 V)	89.8 (40 V)	320	$\sim 10^5$	–	3×10^4	[74]
m-$Zn_{0.39}Mg_{0.61}O$	4 (40 V)	3.7 (40 V)	280	$\sim 10^3$	–	700	[74]

5. Conclusions and perspectives

In this review paper, we present the research progress in the ZnMgO film UV photodetectors developed in recent five years. Abundant achievements can be seen. The classification, performance, and mechanism of ZnMgO photodetectors have been summarized and reviewed. In this review, the ZnMgO photodetectors are divided into three types based on the alloy structure, namely w-ZnMgO, c-ZnMgO, and m-ZnMgO devices, which have been demonstrated using different preparation methods. The performance of ZnMgO photodetector is strongly dependent on the alloy structure. For example, w-ZnMgO photodetector usually has a high responsivity, but its dark current is also very large. In contrast, although the dark current of c-ZnMgO device is very small, its responsivity is low. Interestingly, m-ZnMgO photodetector presents excellent comprehensive performance (lower dark current and higher responsivity) compared with single phase device. Although great progress has been madein ZnMgO UV photodetectors in recent years, the device performance is still far away from the level of practical application. In addition, relatively weak repeatability and also theoretical support still need further improving. Therefore, more work needs to be done in the field of ZnMgO UV photodetectors, such as fabricating the P-type ZnMgO to realize PN-junction devices, improving the responsivity of c-ZnMgO, reducing the dark current of w-ZnMgO, realizing array devices, etc.

References

[1] Chen H Y, Liu K W, Hu L F, Al-Ghamdi A A and Fang X S 2015 *Mater. Today* **18** 493
[2] Peng L, Hu L F and Fang X S 2013 *Adv. Mater.* **25** 5321
[3] Guo F W, Yang B, Yuan Y B, Xiao Z G, Dong Q F, Bi Y and Huang J S 2012 *Nat. Nanotechnol.* **7** 798
[4] Sang L W, Liao M Y and Sumiya M 2013 *Sensors* **13** 10482
[5] Alaie Z, Nejad S M and Yousefi M H 2015 *Mater. Sci. Semicond. Process* **29** 16
[6] You K, Jiang H, Li D B, Sun X J, Song H, Chen Y R, Li Z M, Miao G Q and Liu H B 2012 *Appl. Phys. Lett.* **100** 4
[7] Xie F, Lu H, Chen D J, Ji X L, Yan F, Zhang R, Zheng Y D, Li L and Zhou J J 2012 *IEEE Sens. J.* **12** 5
[8] Zhu D, Wallis D J and Humphreys C J 2013 *Rep. Prog. Phys.* **76** 31
[9] Scholz F 2012 *Semicond. Sci. Technol.* **27** 15
[10] Hardy M T, Feezell D F, DenBaars S P and Nakamura S 2011 *Mater. Today* **14** 408
[11] Cicek E, McClintock R, Cho C Y, Rahnema B and Razeghi M 2013 *Appl. Phys. Lett.* **103** 4
[12] Sedhain A, Lin J Y and Jiang H X 2012 *Appl. Phys. Lett.* **100** 4
[13] Gordon L, Lyons J L, Janotti A and Van de Walle C G 2014 *Phys. Rev. B* **89** 6
[14] Lorenz K, Peres M, Franco N, Marques J G, Miranda S M C, Magalhaes S, Monteiro T, Wesch W, Alves E and Wendler E 2011 *Conference on Oxide-based Materials and Devices II*, January 23–26, 2011, San Francisco, CA, USA
[15] Brillson L J and Lu Y C 2011 *J. Appl. Phys.* **109** 33
[16] Liu K W, Sakurai M and Aono M 2010 *Sensors* **10** 8604
[17] Hou Y N, Mei Z X and Du X L 2014 *J. Phys. D: Appl. Phys.* **47** 25
[18] Yang W, Hullavarad S S, Nagaraj B, Takeuchi I, Sharma R P, Venkatesan T, Vispute R D and Shen H 2003 *Appl. Phys. Lett.* **82** 3424
[19] Makino T, Segawa Y, Kawasaki M, Ohtomo A, Shiroki R, Tamura K, Yasuda T and Koinuma H 2001 *Appl. Phys. Lett.* **78** 1237
[20] Tsukazaki A, Ohtomo A, Kita T, Ohno Y, Ohno H and Kawasaki M 2007 *Science* **315** 1388
[21] Shao R W, Zheng K, Wei B, Zhang Y F, Li Y J, Han X D, Zhang Z and Zou J 2014 *Nanoscale* **6** 4936
[22] Ohtomo A, Kawasaki M, Koida T, Masubuchi K, Koinuma H, Sakurai Y, Yoshida Y, Yasuda T and Segawa Y 1998 *Appl. Phys. Lett.* **72** 2466
[23] Ohtomo A, Tamura K, Kawasaki M, Makino T, Segawa Y, Tang Z K, Wong G K L, Matsumoto Y and Koinuma H 2000 *Appl. Phys. Lett.* **77** 2204
[24] Gruber T, Kirchner C, Kling R, Reuss F and Waag A 2004 *Appl. Phys. Lett.* **84** 5359
[25] Nakahara K, Akasaka S, Yuji H, Tamura K, Fujii T, Nishimoto Y, Takamizu D, Sasaki A, Tanabe T, Takasu H, Amaike H, Onuma T, Chichibu S F, Tsukazaki A, Ohtomo A and Kawasaki M 2010 *Appl. Phys. Lett.* **97** 3
[26] Yang W, Vispute R D, Choopun S, Sharma R P, Venkatesan T and Shen H 2001 *Appl. Phys. Lett.* **78** 2787
[27] Zhu H, Shan C X, Wang L K, Zheng J, Zhang J Y, Yao B and Shen D Z 2010 *J. Phys. Chem. C* **114** 7169
[28] Liu K W, Shen D Z, Shan C X, Zhang J Y, Yao B, Zhao D X, Lu Y M and Fan X W 2007 *Appl. Phys. Lett.* **91** 3
[29] Tabares G, Hierro A, Ulloa J M, Guzman A, Munoz E, Nakamura A, Hayashi T and Temmyo J 2010 *Appl. Phys. Lett.* **96** 3
[30] Tang K, Huang J, Zeng Q K, Zhang J J, Shi W M, Xia Y B and Wang L J 2011 *7th International Conference on Thin Film Physics and Applications*, September 24–27, 2010, Shanghai, China
[31] Li G M, Zhang J W, Liu Y and Zhang K F 2011 *Opt. Eng.* **50** 4
[32] Liu R S, Jiang D Y, Duan Q, Sun L, Tian C G, Liang Q C, Gao S and Qin J M 2014 *Appl. Phys. Lett.* **105** 4

[33] Li J Y, Chang S P, Lin H H and Chang S J 2015 *IEEE Photon. Technol. Lett.* **27** 978

[34] Hwang J D and Lin G S 2016 *Nanotechnology* **27** 6

[35] Hou Y N, Mei Z X, Liang H L, Ye D Q, Liang S, Gu C Z and Du X L 2011 *Appl. Phys. Lett.* **98** 3

[36] Schoenfeld W V, Wei M, Boutwell R C and Liu H Y 2014 *Annual Conference on Oxide-Based Materials and Devices V held at SPIE Photonics West*, February 2–5, 2014, San Francisco, CA, USA

[37] Zhao Y M, Zhang J Y, Jiang D Y, Shan C X, Zhang Z Z, Yao B, Zhao D X and Shen D Z 2009 *ACS Appl. Mater. Interfaces* **1** 2428

[38] Liu K W, Shen D Z, Shan C X, Zhang J Y, Jiang D Y, Zhao Y M, Yao B and Zhao D X 2008 *J. Phys. D: Appl. Phys.* **41** 3

[39] Jiang D Y, Zhang J Y, Liu K W, Zhao Y M, Cong C X, Lu Y M, Yao B, Zhang Z Z and Shen D Z 2007 *Semicond. Sci. Technol.* **22** 687

[40] Hou Y N, Mei Z X, Liang H L, Ye D Q, Gu C Z, Du X L and Lu Y C 2013 *IEEE Trans. Electron Dev.* **60** 3474

[41] Tian C H, Jiang D Y, Tan Z D, Duan Q, Liu R S, Sun L, Qin J M, Hou J H, Gao S, Liang Q C and Zhao J X 2014 *Mater. Res. Bull.* **60** 46

[42] Chen H Y, Liu K W, Chen X, Zhang Z Z, Fan M M, Jiang M M, Xie X H, Zhao H F and Shen D Z 2014 *J. Mater. Chem. C* **2** 9689

[43] Zhao Y J, Jiang D Y, Liu R S, Duan Q, Tian C G, Sun L, Gao S, Qin J M, Liang Q C and Zhao J X 2015 *Solid-State Electron.* **111** 223

[44] Tian C G, Jiang D Y, Pei J A, Sun L, Liu R S, Guo Z X, Hou J H, Zhao J X, Liang Q C, Gao S and Qin J M 2016 *J. Alloys Compd.* **667** 65

[45] Sun L, Jiang D Y, Zhang G Y, Liu R S, Duan Q, Qin J M, Liang Q C, Gao S, Hou J H, Zhao J X, Liu W Q and Shen X D 2016 *J. Appl. Phys.* **119** 5

[46] Hu Z F, Li Z J, Zhu L, Liu F J, Lv Y W, Zhang X Q and Wang Y S 2012 *Opt. Lett.* **37** 3072

[47] Shan C X, Liu J S, Lu Y J, Li B H, Ling F C C and Shen D Z 2015 *Opt. Lett.* **40** 3041

[48] Zhang L N, Lin H T, Wu Y S and Zhuo S P 2016 *Chem. Phys. Lett.* **661** 224

[49] Vempati S, Chirakkara S, Mitra J, Dawson P, Nanda K K and Krupanidhi S B 2012 *Appl. Phys. Lett.* **100** 4

[50] Fan J C, Sreekanth K M, Xie Z, Chang S L and Rao K V 2013 *Prog. Mater. Sci.* **58** 874

[51] Zhang B, Li M, Wang J Z and Shi L Q 2013 *Chin. Phys. Lett.* **30** 027303

[52] Liu L, Xu J L, Wang D D, Jiang M M, Wang S P, Li B H, Zhang Z Z, Zhao D X, Shan C X, Yao B and Shen D Z 2012 *Phys. Rev. Lett.* **108** 5

[53] Liu Z L, Mei Z X, Zhang T C, Liu Y P, Guo Y, Du X L, Hallen A, Zhu J J and Kuznetsov A Y 2009 *J. Cryst. Growth* **311** 4356

[54] Zheng Q H, Huang F, Ding K, Huang J, Chen D G, Zhan Z B and Lin Z 2011 *Appl. Phys. Lett.* **98** 3

[55] Liang H L, Mei Z X, Zhang Q H, Gu L, Liang S, Hou Y N, Ye D Q, Gu C Z, Yu R C and Du X L 2011 *Appl. Phys. Lett.* **98** 3

[56] Hou Y N, Mei Z X, Liang H L, Ye D Q, Gu C Z and Du X L 2013 *Appl. Phys. Lett.* **102** 4

[57] Liang H L, Mei Z X, Hou Y N, Liang S, Liu Z L, Liu Y P, Li J Q and Du X L 2013 *J. Cryst. Growth* **381** 6

[58] Jiang D Y, Tian C G, Yang G, Qin J M, Liang Q C, Zhao J X, Hou J H and Gao S 2015 *Mater. Res. Bull.* **67** 158

[59] Zheng Q H, Huang F, Huang J, Hu Q C, Chen D G and Ding K 2012 *IEEE Electron Dev. Lett.* **33** 1033

[60] Hwang J D, Lin J S and Hwang S B 2015 *J. Phys. D: Appl. Phys.* **48** 6

[61] Wang L K, Ju Z G, Zhang J Y, Zheng J, Shen D Z, Yao B, Zhao D X, Zhang Z Z, Li B H and Shan C X 2009 *Appl. Phys. Lett.* **95** 3

[62] Han S, Zhang J Y, Zhang Z Z, Zhao Y M, Wang L K, Zheng J A, Yao B, Zhao D X and Shen D Z 2010 *ACS Appl. Mater. Interfaces* **2** 1918

[63] Jiang D Y, Shan C X, Zhang J Y, Lu Y M, Yao B, Zhao D X, Zhang Z Z, Shen D Z and Yang C L 2009 *J. Phys. D: Appl. Phys.* **42** 3

[64] Fan M M, Liu K W, Chen X, Zhang Z Z, Li B H, Zhao H F and Shen D Z 2015 *J. Mater. Chem. C* **3** 313

[65] Han S, Zhang Z Z, Zhang J Y, Wang L K, Zheng J, Zhao H F, Zhang Y C, Jiang M M, Wang S P, Zhao D X, Shan C X, Li B H and Shen D Z 2011 *Appl. Phys. Lett.* **99** 4

[66] Boutwell R C, Wei M and Schoenfeld W V 2013 *Appl. Surf. Sci.* **284** 254

[67] Ju Z G, Shan C X, Jiang D Y, Zhang J Y, Yao B, Zhao D X, Shen D Z and Fan X W 2008 *Appl. Phys. Lett.* **9** 3

[68] Xie X H, Zhang Z Z, Li B H, Wang S P, Jiang M M, Shan C X, Zhao D X, Chen H Y and Shen D Z 2014 *Opt. Express* **22** 246

[69] Xie X H, Zhang Z Z, Li B H, Wang S P and Shen D Z 2015 *Opt. Express* **23** 32329

[70] Boutwell R C, Wei M and Schoenfeld W V 2013 *Appl. Phys. Lett.* **103** 4

[71] Liu C Y, Xu H Y, Wang L, Li X H and Liu Y C 2009 *J. Appl. Phys.* **106** 4

[72] Xie X H, Zhang Z Z, Shan C X, Chen H Y and Shen D Z 2012 *Appl. Phys. Lett.* **101** 3

[73] Fan M M, Liu K W, Zhang Z Z, Li B H, Chen X, Zhao D X, Shan C X and Shen D Z 2014 *Appl. Phys. Lett.* **10** 5

[74] Fan M M, Liu K W, Chen X, Wang X, Zhang Z Z, Li B H and Shen D Z 2015 *ACS Appl. Mater. Interfaces* **7** 20600